A. PALANISAMY*, T. SELVARAJ*, S. SIVASANKARAN**#

EXPERIMENTAL INVESTIGATION AND MULTI-RESPONSE OPTIMIZATION IN TURNING OF INCOLOY 800 H SUPERALLOY

This research work is focused on examining the turning behavior of Incoloy 800H superalloy by varying important cutting parameters. Incoloy 800H is an Iron- Nickel-Chromium based superalloy; it can withstand high temperature (810°C), high oxidization and corrosion resistance. But, it is difficult to turn in conventional machines and hence the present work was carried out and investigated. Experiments were conducted based on the standard L_{27} orthogonal array using uncoated tungsten inserts. The cutting force components, namely, feed force (Fx), thrust force (Fy) and cutting force (Fz); surface roughness (Ra) and specific cutting pressure (SCPR) were measured as responses and optimized using Taguchi-Grey approach. The main effects plots and analysis of mean (*ANOM*) were performed to check the effect of turning parameters and their significance on responses of cutting forces in all the direction (F_X, FY, FZ), the surface roughness (*Ra*) and specific cutting pressure (*SCPR*). The tool wear and machined surfaces were also investigated using white light interferometer and SEM.

Keywords: Superalloy; Microstructure; Taguchi- Grey approach; mathematical models

1. Introduction

The design and development of high-temperature components would need high strength at elevated temperature, high resistance to wear, high resistance to corrosion and more in chemical stability. These properties can be achieved by Nickel based superalloys nowadays and its applications including aerospace, space, marine etc are being used [1]. Conversion of this super-alloy into required components would need machining process. Among several Nickel based alloys such as Nickel 200, Monel 400, Nickel 600, Incoloy 800, Hastelloy and Zirconium alloy, Incoloy 800 H is recently taken as one of the important materials in all fields especially in aerospace industries [2]. In aerospace industries, about 50% of the gas-turbine engines are made up of superalloys [3]. Superalloys are hard machining materials due to rapid hardening, with massive strength at higher temperature, the affinity of chips in the direction of cutting boundaries and low thermal conductivity [4]. Superalloys are extremely admired in the manufacturing sectors owing to their advantages more than titanium alloys because of their supreme properties at high temperature [5]. Since the forces required for cutting super alloys are about two times greater than necessary for alloy steels due to rapid hardening, Incoloy 800H also work fast -hardens during machining. Based on several literature [6-9], it can be understood that proper selection of turning parameters is very much important in the manufacturing industries to have good aesthetic machined components.

In advanced manufacturing industries, turning operation is an important and common one in which the turned surface of the component mainly depends on cutting parameters; condition of cutting inserts and materials which influence the process capability. In general, the selections of parameters for machining are mainly based on operator's experiences, knowledge, and skills in addition to parameters prescribed by the standard handbooks [10]. However, the selected process parameters as mentioned in the standard handbook could not be the best solution because it is mainly defined by chemical composition. In actual practice, the machining behavior would mainly depend on chemical composition, hardness, selection of cutting parameters, tool materials, tool condition and heat treatment etc… [10]. These parameters would influence the machining forces produced during turning that directly affect the quality of the component and tool life. The value of surface roughness to be obtained during machining would define the surface quality of the component which mainly depends on the corrosion resistance, wear resistance and fatigue strength of the material [11,12]. Further, the tool conditions such as coated and uncoated tool inserts would define the quality of the machined component. In general, harder materials would experience more amount of turning forces [13,14] which need more and clear investigation in order to have the machined component as per customer expectation. In addition, one more response to specific cutting pressure (SCPR) is also important as it helps to determine the spindle input power for machining/turning the material. SCPR is the pressure acting in

* NATIONAL INSTITUTE OF TECHNOLOGY, DEPARTMENT OF PRODUCTION ENGINEERING, TIRUCHIRAPPALLI - 620 015, TAMILNADU, INDIA
** QASSIM UNIVERSITY, DEPARTMENT OF MECHANICAL ENGINEERING, COLLEGE OF ENGINEERING, BURAIDAH, SAUDI ARABIA

Corresponding author: sivasankarangs1979@gmail.com, sivasankaran@qec.edu.sa

the cutting direction during machining/turning unit area in mm with a thickness of 1mm which the value depends on materials and its properties [15]. The selection of cutting insert and their machining performance assessment have forever a big challenge to the manufacturers [16]. Dry machining is widely used in manufacturing industries which diminish the overhead costs and protect the environment from pollution [17]. The turning behavior of AISI D2 cold work tool steel and AISI 4340 steel were explored by Lima et al. [18] in which good surface finish was acquired at a higher value of cutting speed. Further, the authors were reported that the surface finish of turned component was affected with increasing of feed rate. The hard turning behavior of AISI 4340 steel was investigated by Suresh et al. [6] in which the authors were revealed that higher cutting forces and poor in surface finish were obtained at low cutting speed, high feed rate and high depth of cut due to higher value of coefficient of friction between work material and cutting tool. Aouici et al. [7] investigated the turning behaviour of AISI H11 steel and reported that the measured cutting forces were more when the hardness of work material started to increases. Further, the cutting forces and surface finish had depended on cutting speed followed by the depth of cut. Kumar et al. [8] examined the turning behavior of martensitic stainless steel using alumina-based ceramic tools and reported that less amount of tool wear had occurred while turning of martensitic stainless steel using alumina mixed TiC and TiN ceramic tools. This was attributed to immediate metal shearing action occurred between coated inserts and hard work material. The improvement in surface finish and decreasing of tool wear with the function of turning parameters were explored by Thamizhmanii et al. [9] while studying of turning of AISI 8620 steel. The authors were reported and observed that reduction in tool wear and excellent surface finish were obtained at lower turning parameters due to less diffusion of work material at these operating parameters and built up edge formation was almost nil over the inserts.

The current research was aimed towards the optimizing the turning parameters of Incoloy 800H in dry condition to protect the environment from pollution (without the use of chemical coolants). The chemical composition and microstructure of as-received Incoloy 800 H superalloy were examined using microscopes. The uncoated tungsten carbide inserts were used in this research to avoid delamination problems at the higher temperature (unavoidable in coated tools). For optimizing the process parameters, Grey-Taguchi hybrid methods was projected and studied to convert multi-response objective functions into the single objective function. Many researchers have taken efforts to expand the plan of experiments for optimization using Grey-Taguchi method on the basis of OA [19,20].

2. Materials and methods

Incoloy 800H material in rod forms of 120 mm length with 25 mm diameter was purchased from Pearl Steel Industries, Mumbai, India. The chemical composition and the sample prepa-

ration were explained in our previous work [21,22]. The proper metallographic procedure was carried out to have the effective microstructure and orientation of grain sizes. Optical microscope (OLYMPUS, Chennai, India) with image analyzer was used to see the microstructure of as-received Incoloy 800H. Scanning electron microscope (SEM, SU3500-Hitachi) with energy dispersive analysis (EDAX) was also carried out to check the chemical composition of as-received Incoloy 800H super-alloy, machined samples, and tool profile.

The computer numerical controlled (CNC) turning experiments were conducted without cutting fluid (dry environment). The Leadwell CNC turning Centre [22] was used in which the set maximum spindle speed was 4500 rpm and the input power used was 7.5 kW. Standard L_{27} orthogonal array (OA) had used for the experimentation [23]. Table 1 shows the input independent and controlled cutting parameters with its level. The tungsten carbide (WC) inserts (ISO *K20, CNMA 120408-THM*, WIDIA, India) and an ISO labeled *PCLNL 1610 M12* tool holder was used during turning. The measured tungsten carbide (WC) turning tool geometry composed of clearance angle was 5°, side rake angle was –6°, inclination angle was –6°, approach angle was 95°, point angle was 80° and nose radius was 0.8 mm. The three turning forces were measured using Kistler type piezoelectric dynamometer (9257B, Switzerland) and the surface finish in terms of surface roughness (Ra) was measured using Mitutoyo SJ 411 surf tester. Further, three dimensional (3D) surface profilometer (Rtec Instrument, USA) was used to examine the topography of machined samples using the white light interferometer. The planned experiments results were conducted as per well-known Taguchi design of experiments and optimized the various responses using grey relational analysis. The detailed well known Taguchi quality characteristics and the procedure for grey-relational analysis were explained elsewhere [21]. The observed experimental results and the corresponding signal-to-noise (S/N) ratio are presented in Table 2.

TABLE 1

Controllable turning parameters and their levels

Symbols	Factors	Level 1	Level 2	Level 3
$A = Vc$	Cutting speed (m/min)	35	45	55
$B = f$	Feed rate (mm/rev)	0.02	0.04	0.06
$C = ap$	Depth of cut (mm)	0.5	0.75	1

3. Results and discussions

3.1. Microstructural examination and machined samples results

The microstructure and grain size with its orientation of as-received Incoloy 800H super-alloy is important before investigating the machining behavior for a better understanding of the readers. The optical microstructure of as-received Incoloy 800H is shown in Fig. 1a. It was noted from several optical images that

Measured responses and their corresponding S/N ratio

| Sl.No	Responses					S/N ratio *(dB)*				
	FX (N)	*FY* (N)	*FZ* (N)	*Ra* (μm)	*SCPR* (N/mm²)	*FX*	*FY*	*FZ*	*Ra*	*SCPR*
1	103.2	151.6	223.1	1.49	22310.00	–40.27	–43.61	–46.97	–3.46	–86.97
2	114.3	167.5	323.6	1.50	21573.33	–41.16	–44.48	–50.20	–3.52	–86.68
3	124.7	177.9	385.01	1.52	19250.50	–41.92	–45.00	–51.71	–3.64	–85.69
4	110.3	180.6	339.3	1.61	16965.00	–40.85	–45.13	–50.61	–4.14	–84.59
5	122.51	186.9	421.9	1.63	14063.33	–41.76	–45.43	–52.50	–4.24	–82.96
6	134.1	190.3	510.3	1.65	12757.50	–42.55	–45.59	–54.16	–4.35	–82.12
7	118.2	196.4	416.29	1.73	13876.33	–41.45	–45.86	–52.39	–4.76	–82.85
8	129.2	206.5	479.3	1.76	10651.11	–42.23	–46.30	–53.61	–4.91	–80.55
9	140.1	210.6	551.9	1.78	9198.33	–42.93	–46.47	–54.84	–5.01	–79.27
10	81.4	126.9	168.7	1.39	16870.00	–38.21	–42.07	–44.54	–2.86	–84.54
11	93.88	137.6	223.6	1.42	14906.67	–39.45	–42.77	–46.99	–3.05	–83.47
12	104.5	155.3	312.74	1.44	15637.00	–40.38	–43.82	–49.90	–3.17	–83.88
13	88.9	148.8	206.97	1.51	10348.50	–38.98	–43.45	–46.32	–3.58	–80.30
14	100.2	157.1	321.9	1.54	10730.00	–40.02	–43.92	–50.15	–3.75	–80.61
15	110.8	171.4	396.24	1.55	9906.00	–40.89	–44.68	–51.96	–3.81	–79.92
16	95.4	163.4	280.15	1.64	9338.33	–39.59	–44.27	–48.95	–4.30	–79.41
17	107.17	174.6	386.66	1.66	8592.44	–40.60	–44.84	–51.75	–4.40	–78.68
18	117.3	183.4	479.31	1.67	7988.50	–41.39	–45.27	–53.61	–4.45	–78.05
19	68.3	124.6	178.7	1.29	17870.00	–36.69	–41.91	–45.04	–2.21	–85.04
20	73.9	136.7	180.8	1.32	12053.33	–37.37	–42.72	–45.14	–2.41	–81.62
21	84.6	134.6	147.9	1.34	7395.00	–38.55	–42.58	–43.40	–2.54	–77.38
22	62.4	139.5	262.86	1.41	13143.00	–35.90	–42.89	–48.39	–2.98	–82.37
23	79.9	140.6	212.5	1.43	7083.33	–38.05	–42.96	–46.55	–3.11	–77.00
24	88.6	153.6	287.4	1.45	7185.00	–38.95	–43.73	–49.17	–3.23	–77.13
25	75.76	133.6	211.3	1.53	7043.33	–37.59	–42.52	–46.50	–3.69	–76.96
26	85.42	142.6	259.51	1.56	5766.89	–38.63	–43.08	–48.28	–3.86	–75.22
27	95.56	158.6	388.9	1.57	6481.67	–39.61	–44.01	–51.80	–3.92	–76.23
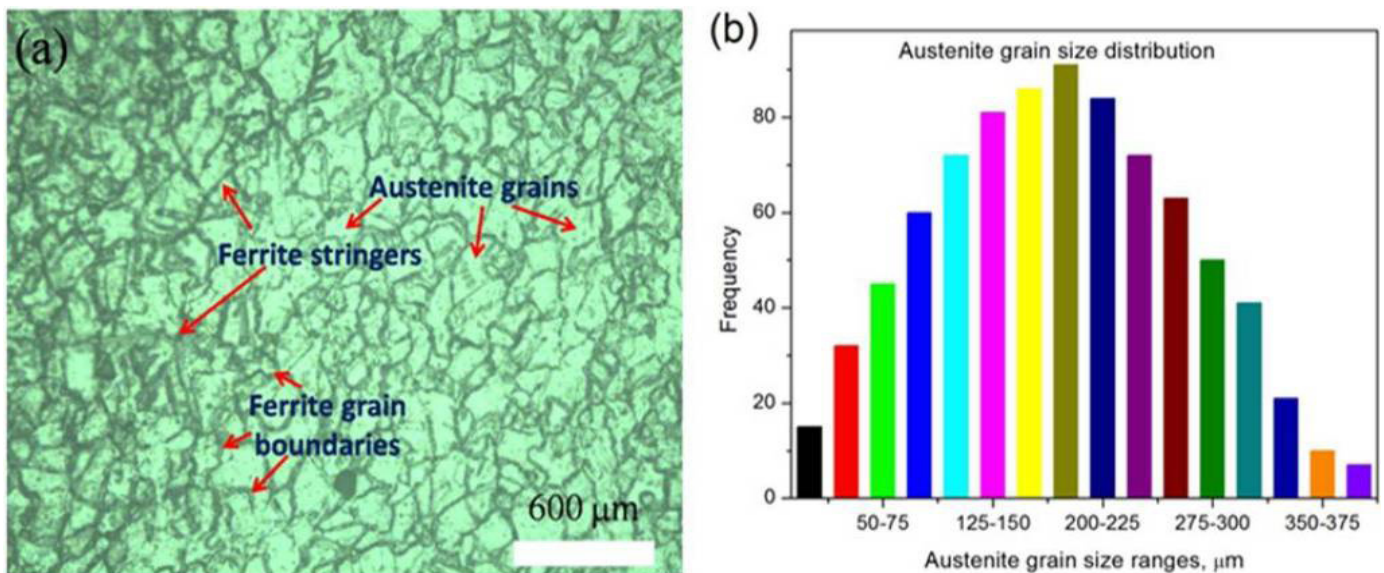
Fig. 1. (a) Optical microstructure of as-received Incoloy 800H; (b) grain size distribution

austenite equiaxed grains were observed and ferrite grain boundaries with ferrite stringers were also observed in some places. The presence of ferrite stringers would enhance the strength and ductility of Incoloy 800H and hence, it ultimately improves the toughness of the material. Here, linear intercept method was used to calculate the average grain sizes in which 833 grains were counted with different grain size ranges. The observed average grain size was 182 mm. The grain size distribution is also shown

Normalized data, Grey relational coefficient, Grade and Rank

Ex. No.	Normalized data					Grey relational coefficient					Grade	Rank
	FX	FY	FZ	Ra	SCPR	FX	FY	FZ	Ra	SCPR		
1	0.475	0.686	0.814	0.592	0.000	0.488	0.614	0.729	0.551	0.333	0.543	15
2	0.332	0.501	0.565	0.571	0.045	0.428	0.501	0.535	0.538	0.344	0.469	20
3	0.198	0.380	0.413	0.531	0.185	0.384	0.447	0.460	0.516	0.380	0.437	22
4	0.384	0.349	0.526	0.347	0.323	0.448	0.434	0.513	0.434	0.425	0.451	21
5	0.226	0.276	0.322	0.306	0.498	0.393	0.408	0.424	0.419	0.499	0.429	23
6	0.077	0.236	0.103	0.265	0.577	0.351	0.396	0.358	0.405	0.542	0.410	26
7	0.282	0.165	0.336	0.102	0.510	0.410	0.375	0.429	0.358	0.505	0.415	24
8	0.140	0.048	0.180	0.041	0.705	0.368	0.344	0.379	0.343	0.629	0.412	25
9	0.000	0.000	0.000	0.000	0.793	0.333	0.333	0.333	0.333	0.707	0.408	27
10	0.755	0.973	0.949	0.796	0.329	0.672	0.949	0.907	0.710	0.427	0.733	6
11	0.595	0.849	0.813	0.735	0.448	0.552	0.768	0.727	0.653	0.475	0.635	11
12	0.458	0.643	0.592	0.694	0.403	0.480	0.583	0.551	0.620	0.456	0.538	16
13	0.659	0.719	0.854	0.551	0.723	0.594	0.640	0.774	0.527	0.644	0.636	10
14	0.514	0.622	0.569	0.490	0.700	0.507	0.570	0.537	0.495	0.625	0.547	14
15	0.377	0.456	0.385	0.469	0.750	0.445	0.479	0.449	0.485	0.666	0.505	18
16	0.575	0.549	0.673	0.286	0.784	0.541	0.526	0.604	0.412	0.698	0.556	13
17	0.424	0.419	0.409	0.245	0.829	0.465	0.462	0.458	0.398	0.745	0.506	17
18	0.293	0.316	0.180	0.224	0.866	0.414	0.422	0.379	0.392	0.788	0.479	19
19	0.924	1.000	0.924	1.000	0.268	0.868	1.000	0.868	1.000	0.406	0.828	1
20	0.852	0.859	0.919	0.939	0.620	0.772	0.780	0.860	0.891	0.568	0.774	3
21	0.714	0.884	1.000	0.898	0.902	0.636	0.811	1.000	0.831	0.836	0.823	2
22	1.000	0.827	0.715	0.755	0.554	1.000	0.743	0.637	0.671	0.529	0.716	7
23	0.775	0.814	0.840	0.714	0.920	0.689	0.729	0.758	0.636	0.863	0.735	5
24	0.663	0.663	0.655	0.673	0.914	0.597	0.597	0.592	0.605	0.854	0.649	9
25	0.828	0.895	0.843	0.510	0.923	0.744	0.827	0.761	0.505	0.866	0.741	4
26	0.704	0.791	0.724	0.449	1.000	0.628	0.705	0.644	0.476	1.000	0.691	8
27	0.573	0.605	0.403	0.429	0.957	0.540	0.558	0.456	0.467	0.920	0.588	12

in Fig. 1b which ensure the uniform distribution. The calculated grey relational grade (GRG) on machined samples is illustrated in Table 3. It was observed that nineteenth trial (Table 3, Ex. No 19) has the largest GRG value (optimum one) and the lowest GRG was obtained in Ex.No 9 (A1B3C3, worst one). Therefore, the observed best optimum turning parameters for Incoloy 800H were *A3B1C1* based on mean response value and GRG which was two times higher than the worst one (Ex. No 9) (Table 3 and Table 4). These results explained that minimum cutting force components and better surface finish (Table 2) were obtained at a higher cutting speed of 55 mm/min, the lower feed rate of 0.02 mm/min and lower depth of cut of 0.5 mm. These similar outcomes were obtained by Suresh et al. [24] while investigating

TABLE 4

Mean response table for Grey relational grade

Level	Cutting speed (V)	Feed (f)	Depth of cut (a)
	A	B	C
1	0.4417	**0.6423**	**0.6243**
2	0.5705	0.5641	0.5775
3	**0.7272**	0.5329	0.5375
Delta	0.2855	0.1094	0.0868
Rank	1	2	3
Optimal combination condition is *A3B1C1*			

the machining behavior of AISI 4340 steel. The *ANOM* was also performed for the multi-response characteristics and the values have been reported in Table 5. Hence, the cutting parameter combination of A3B1C1 could be best suited for machining of Incoloy 800H which would be helpful in advanced manufacturing industries.

3.2. Effect of turning parameters on cutting force components (F_X, F_Y and F_Z)

The measured three orthogonal turning forces (*Fx*, *Fy* and *Fz*) turned at different input parameters are given in Table 2. Fig. 2a-c show the variation of main effect plots on three forces with the function of turning parameters. In general, three orthogonal cutting components would start to increases (Fig. 2) when the value of feed rate and value of a depth of cut increases. This is the fact due to strain-hardening effect usually occur between work material and cutting tool during metal cutting; and the amount of material removal rates which depend on turning parameters [25]. As the feed rate had started to increases, the quantity of material get in touch with the cutting tool also increases. Due to this, the contact length of tool-work would start to increases and hence the cutting force component also increases.
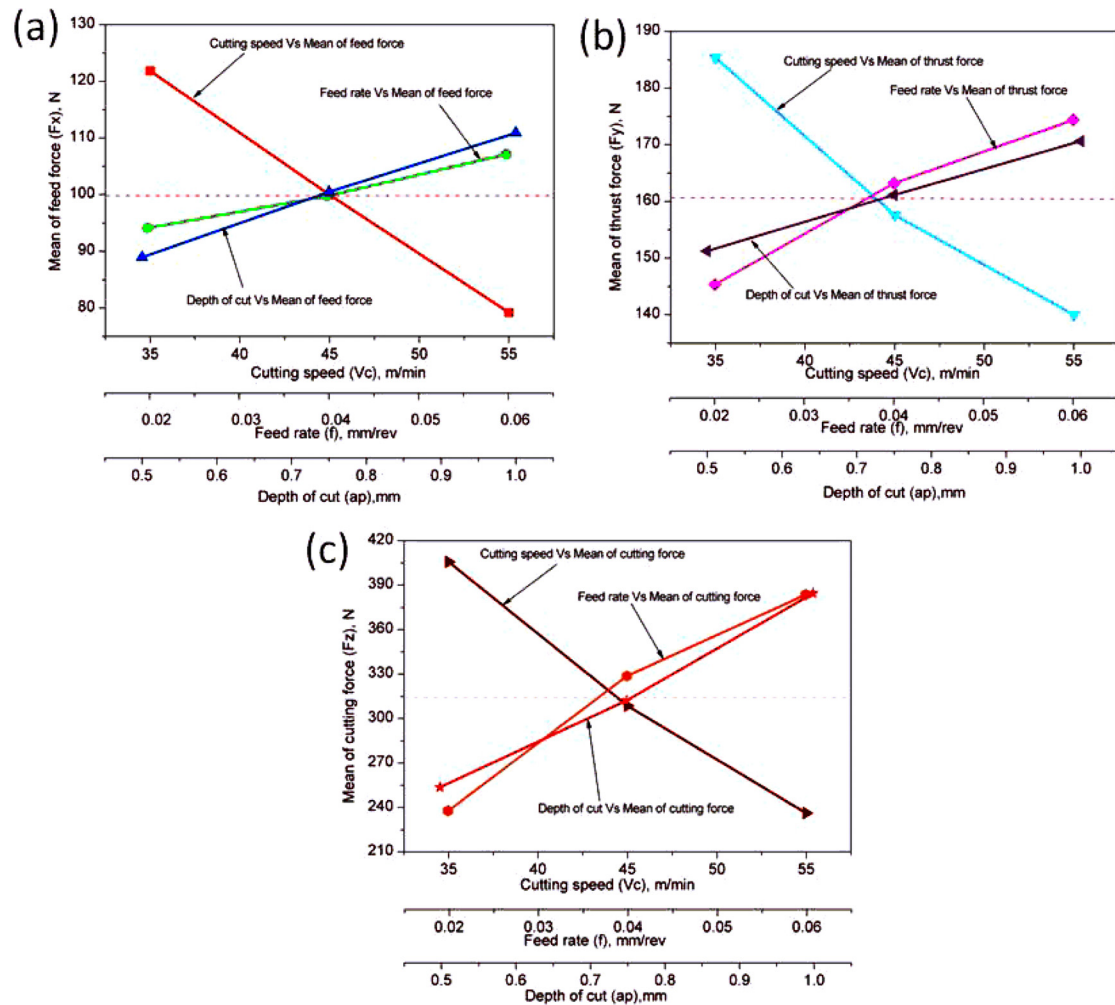
Fig. 2. Variation of main effect plots of various machining forces with function of turning parameters: (a) feed force; (b) thrust force; (c) cutting force

Further, these increased turning forces with the function of feed and depth of cut were attributed to more friction between the work and tool [25]. It was noted here that the highest values of three turning forces (Fx, Fy and Fz, Table 2) were obtained at a lower value of cutting speed of 35 m/min, high value of feed rate (0.06 mm/rev) and high value of a depth of cut (1 mm). In addition, it was observed from the experimental investigations that the ranges of cutting force components values were $F_X =$ 62.4N-140.1N, $F_Y =$124.6N-210.6N and $F_Z =$ 147.9N-551.9N obtained for various machining conditions. The optimal turning force components ($F_X =$ 68.3N, $F_Y =$ 124.6N, and $F_Z =$ 178.76N) were obtained at $f =$ 0.02 mm/rev, at $ap =$ 0.5 mm, at $Vc =$ 55 m/min. These results explained that higher amount of cutting force components were observed at lower cutting speed, higher feed rate and higher depth of cut (Ex. No 9) which was 2.66 times higher than the optimal condition. The same result phenomenon was obtained by Senthil et al. [26] while machining of Al-Cu/TiB$_2$ in-situ metal matrix composites produced through liquid metallurgy route. Further, the cutting force components values were started to reduce while increasing the value of cutting speed from 35 to 55 m/min owing to higher temperature produced which induce thermal softening of work sample during machining [27,28]. In overall, based on Fig. 2a-c, it can be ob-

served further that all the three cutting force components were considerably affected by the cutting speed (more deviation from the mean, Fig. 2) followed by feed rate and depth of cut. Similar kind of behavior was observed by Aouici et al. [7] while studying the turning behavior of AISI H11 hardened steel using carbon boron nitride (CBN) tool.

3.3. Effect of turning parameters on surface roughness (*Ra*)

Table 2 shows the observed values of surface roughness turned using different turning parameters. The variation of surface roughness on several turning parameters in the form of main effect plot is shown in Fig. 3a. It was identified here that the feed rate was the highly significant parameter which affects the value of surface roughness considerably. It is the fact that the surface quality of the turned workpiece could depend on cutting conditions which define the fatigue life of machined components. Due to this, the investigation on the variation of surface roughness by varying turning parameters was carried out in the present research work. The surface roughness measurement was carried out on three locations of turned surface of

the workpiece. In each experiment, the measurement was taken thrice and the average values were used for investigation which is reported in Table 2. It was noticed that the surface roughness was started to increases as the feed rate increases from 0.02 to 0.06 mm/rev, which was caused by increased metal removal rate (*MRR*) at a definite speed (Fig. 3a). The increased surface roughness values with the function of feed rate were attributed to increasing the amount of friction between work materials and turning tool [25]. Also, it was noticed that surface roughness value was started to decreases by increasing the value of cutting speed which was owing to thermal softening of materials [27,29]. The observed values of surface roughness ranges were from 1.29 μm to 1.78 μm. For optimal machining conditions, the surface roughness (*Ra)* value was 1.29μm whereas it was 1.78 μm for worst condition (Ex. No 9) which was 1.4 times higher than the optimum one (Ex. No 19). From Fig. 3a, it was clear that the surface roughness was significantly affected by the function of feed rate (more deviation from the mean) followed by cutting speed (average deviation from the mean) and depth of cut (less deviation from mean). Increasing the value of surface roughness with feed rate and decreasing the value of surface roughness with cutting speed were also observed and examined by Senthil et al. [26] and Das et al. [27].

3.4. Effect of turning parameters on specific cutting pressure (*SCPR*) and grey relational grade (GRG)

The observed values of specific cutting pressure (SCPR) with the function of different turning parameters are listed in Table 2. The main effect plot on the variation of SCPR as a function of turning process parameters is shown in Fig. 3b. The observed results had indicated that both the cutting speed and feed rate were influenced more on SCPR as a function of process parameters. The *SCPR* principally depends on the area of the chip ($f \times ap$). The combination of feed and depth of cut; and deviation of cutting force components from the mean would define different chip cross section which influences the amount of SCPR during turning/machining of material [30,31]. The formation of cutting edge between work material and tool during machining would define the surface quality of the component. This feature of cutting edge would indirectly affect the amount of SCPR. The *SCPR* was projected from the measured cutting force (F_Z) for all the machining conditions using Eq (1):

$$SCPR = FZ/A = FZ/f * ap \text{ (N/mm}^2) \tag{1}$$

Where F_Z is the observed amount of cutting force, and A is the area of uncut chip cross-section ($f * ap$). Generally, the *SCPR*
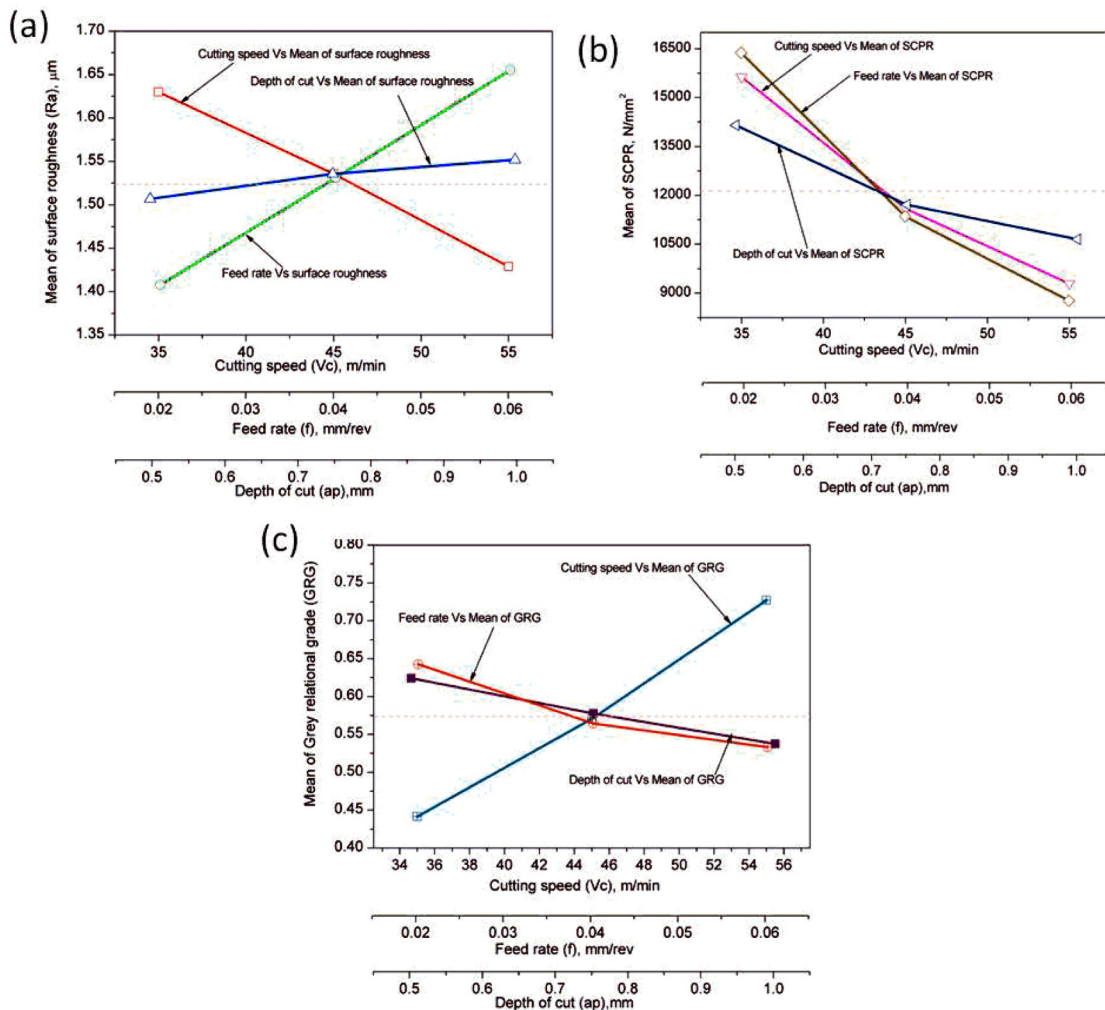

Fig. 3. Variation of main effect plots with function of turning parameters: (a) surface roughness; (b) specific cutting pressure; (c) grey relational grade

varies with respect to different turning parameters. The material was subjected to lower strain rate while turning at a lower value of feed rate. The *SCPR* was started to decrease when the cutting speed increases which results in a reduction of shear strength owing to increase of temperature in the machining region. The range of SCPR from the experiments was 5766.887 N/mm^2 – 22310 N/mm^2 for various machining conditions. The observed minimum SCPR was 5766.89 N/mm^2 (Ex. No 26) which would help us to save the energy consumption while machining of Incoloy 800H by the industrial people. After converting the multi responses into single response based on the value of GRG by Taguchi-grey theory (Table 3), the main effect plot on GRG as a function of turning parameters was plotted and the same is shown in Fig. 3c. From Fig. 3c, it was observed that the overall GRG was significantly affected by cutting speed (more deviation from the mean) followed by feed rate (average deviation from the mean) and depth of cut (less deviation from mean). The range of GRG as a function of turning parameters is 0.408 to 0.828. The higher value of GRG would give better turning behavior (Ex. No 19) whereas lower value would produce worst turning behavior (Ex. No 9).

3.5. SEM and EDX analysis for tool wear and machined surface

The crater wear occurred in tool for the worst cutting condition of A1B3C3 (Ex. No. 09) is shown in Fig. 4a. It was noticed here on the rake surface that the blended adhesive and diffusion mechanisms had played a major role on the tool wear. This was attributed to high temperature induced between work material and tool rake face. Further, crater wear might have occurred by sliding friction caused by the chips over the rake face of the tool consequently some chips would start to stick over the rake face that promotes more friction [10]. To explicate diffusion at

the tool-chip interfaces, an EDX analysis was conducted on the crater surface of the cutting insert which is shown in Fig. 4b. Similarly, Fe, Ni, Cr, Ti, Al, and Mg contents were good indicators for material transferred from work material to cutting insert rake face during turning operations. The 3D surface profile on turned surface is shown in Fig. 5a and Fig. 5b for Exp. No 19 (best condition), and Exp. No 09 (worst condition) respectively which were taken by high-resolution white light interferometer. Here, the surface topography defines the surface roughness on the surface. High amplitude topography in the form of peak and valley was observed in the sample which had more surface roughness value (Ex. No. 09, Fig. 5b). It was clearly observed that in optimal cutting condition (Fig. 5a), Exp. No. 19; very less amplitude topography was observed which means good surface in the workpiece. Based on Fig. 5 results, the corresponding SEM images on machined surfaces were also carried out and the same is shown in Fig. 6a-b for Exp. No 19 (best condition), and Exp. No 09 (worst condition) respectively. More amounts of feed marks could be observed on the turned/machined surface on Exp. No. 9 (Fig. 6b) which was the worst condition. Further, the surface contains more pit holes and tiny cracks, which are unevenly distributed on the turned surface, could be observed from SEM image of Fig. 6b. However, an almost negligible quantity of feed markers with zero pits could be observed in the optimal setting combination (*A3B1C1*) (Fig. 6a).

3.7. Confirmation experiment for turning of Incoloy 800H

The confirmation test was conducted in order to check whether the obtained optimum cutting condition would have improved performance or not.

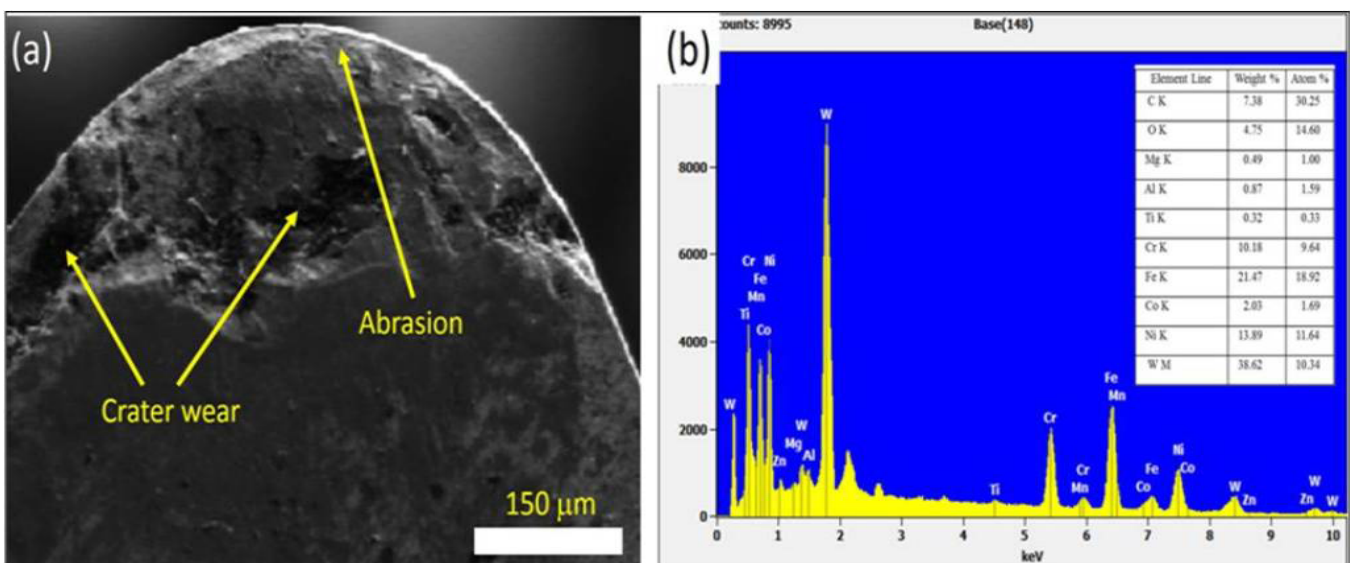The confirmation trials were performed, to confirm the enhancement of performance characteristics by the obtained

Fig. 4. Tool wear surface analysis of untreated CNMA WC tool of Ex. No. 09: (a) SEM image on tool tip; (b) corresponding EDAX analysis on tool tip
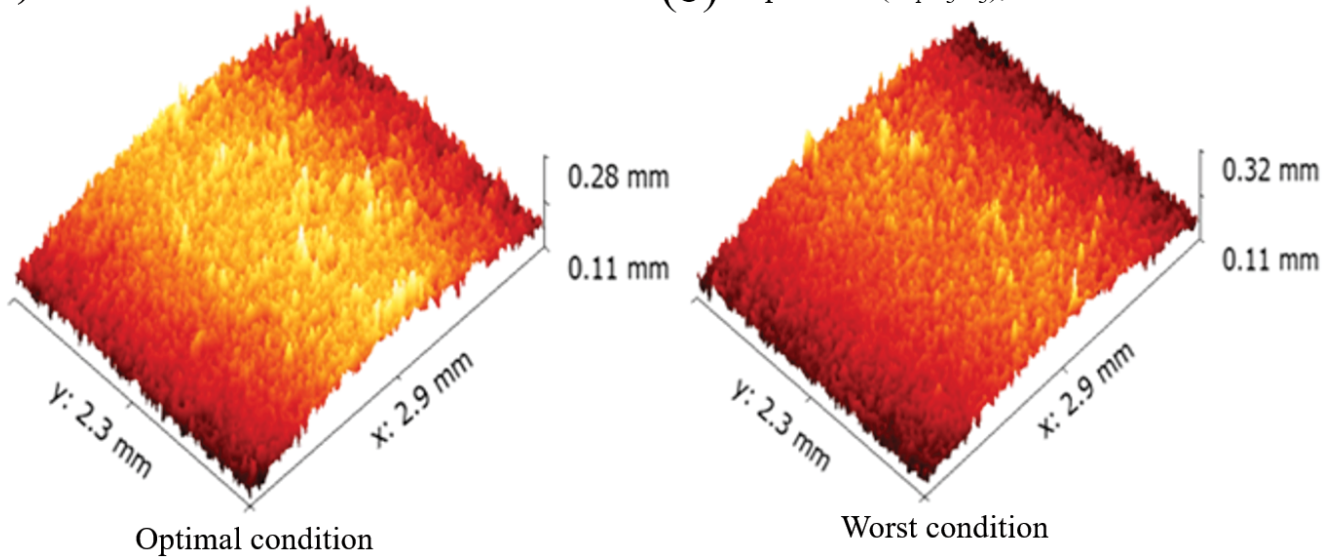
1690

Fig. 5. Variation of surface roughness 3D profile: (a) Exp. No 19; (b) Exp. No 09
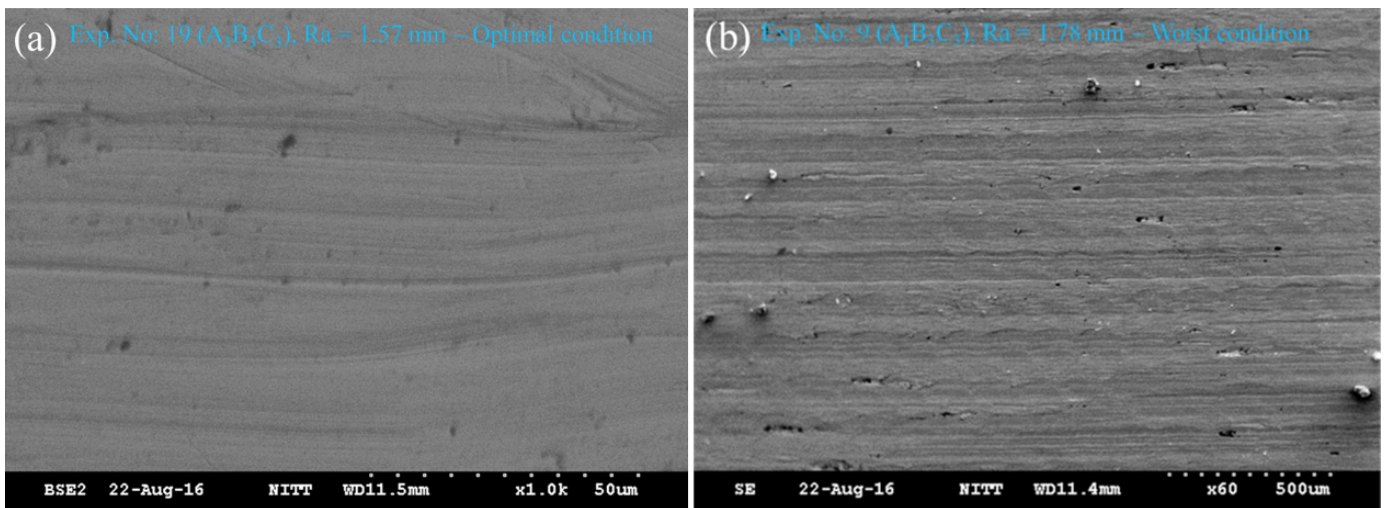

Fig. 6. SEM images on machined surfaces: (a) Exp. No 19; (b) Exp. No 9

optimal level of turning parameters. The estimation or prediction of GRG can be determined using the following expression [10,13]:

$$\gamma_{estimated} = \gamma m + \sum_{i=1}^{n}(\gamma i - \gamma m) \qquad (2)$$

Where γn is the total mean of GRG, γi is GRG average at the optimal condition by which the significant parameters of A, B and C can be determined; n is the number of parameters which considerably influence the quality characteristics. Table 6 shows the results of confirmation tests in which three trials were conducted and the average was taken for investigation. It was observed from Table 5 that the performance improvement at optimal condition around 57.45% was improved when compared to the initial condition. Further, the Table 6 revealed that the feed force (Fx) was started to decreases from 103.2 N to 66.9 N; the thrust force (Fy) was reduced from   151.6 N to 120.4 N; the

cutting force started to decrease 174.38 N from 223.1 N; the surface roughness value decreased from 1.49 mm to 1.25 mm; and the *SCPR* reduced from 22310 N/mm^2 to 17438 N/mm^2.

TABLE 5

Results of Analysis of mean (ANOM) for multi-performance characteristics

Levels	Mean			S/N ratio		
	Cutting speed (Vc), m/min	Feed rate (f), mm/rev	Depth of cut (ap), mm	Cutting speed (Vc), m/min	Feed rate (f), mm/rev	Depth of cut (ap), mm
1	0.4382	0.6286	0.6160	−7.1957	−4.2557	−4.4174
2	0.5609	0.5559	0.5673	−5.0870	−5.2786	−5.1207
3	0.7138	0.5284	0.5297	−2.9750	−5.7234	−5.7195
Delta	0.2755	0.1002	0.0863	4.2207	1.4677	1.3021
Rank	1	2	3	1	2	3

TABLE 6

Results of the Confirmation Experiment

Levels	Initial conditions	Optimal cutting conditions	
		Prediction	Experiment
	A1B1C1	A3B1C1	A3B1C1
FX, N	103.2		66.9
FY, N	151.6		120.4
FZ, N	223.1		174.38
Ra, μm	1.49		1.25
SCPR, N/mm^2	22310		17438
GRG	0.533	0.828	0.839
The improvement in GRG = 0.306		The percentage improvement in GRG = 36.47%	

4. Conclusions

The Grey-Taguchi optimization methods were successfully used and identified the optimal machining parameters for multi responses of Incoloy 800H superalloy during dry turning operations. The following specific conclusions were drawn from this research work:

- The microstructure of as-received Incoloy 800H superalloy was effectively characterized using microscopes and the chemical composition was checked by energy dispersive spectroscopy analysis
- Based on the higher value of GRG and confirmation test, it was identified the optimum turning parameters to machine the Incoloy 800H super alloy which was 55 m/min of cutting speed, 0.02 mm/rev of feed rate and 0.5 mm of a depth of cut. These turning parameters were exhibited the reduction in turning forces, good surface finish, and minimum SCPR
- In overall GRG, the high influence parameter on all the responses was cutting speed followed by feed rate and depth of cut.
- The higher amount of cutting force components was obtained when increasing both feed rate and depth of cut. This was attributed to more amount of friction produced between tool and work material. However, the observed cutting force components were started to decreases by increasing the cutting speed due to thermal softening.
- The good surface finish was obtained at a higher amount of cutting speed, a lower amount of feed rate and lower amount of depth of cut. The minimum specific cutting pressure was obtained at a higher value of cutting speed, a higher level of feed rate and middle-level depth of cut.
- The formation of tool wear was occurred due to adhesive and diffusive mechanics at the rake face, crater wear and some grooves created by sliding friction of chips over the rake face. More feed marks; and sharp peak and valley were observed in initial condition whereas it was minimum at optimum condition.

REFERENCES

[1] E.O. Ezugwu, Int. J. Adv. Manuf. Technol. **45** (12-13), 1353-1367 (2005).

[2] W. Ren, R. Swindeman, J Press Vess-T Asme. **136** (5), 054001-0540012 (2014).

[3] K. Venkatesan, R. Ramanujam, P. Kuppan, Opt. Laser. Technol, **78**, 10-18 (2016).

[4] D. Ulutan, T. Ozel, Int. J. Mach. Tool. Manu, **51** (3), 250-280 (2011).

[5] B. Davoodi, B. Eskandari, Measurement **68**, 286-294 (2015).

[6] R. Suresh, S. Basavarajappa, G.L. Samuel, Measurement **45** (7), 1872-1884 (2012).

[7] H. Aouici, M.A. Yallese, K. Chaoui, T. Mabrouki, J.F. Rigal, Measurement. **45** (3), 344-353 (2012).

[8] A.S. Kumar, A.R. Durai, T. Sornakumar, J. Mater. Process. Technol. **173** (2), 151-156 (2006).

[9] S. Thamizhmanii, K. Kamarudin, E.A. Rahim, A. Saparudin, S. Hassan, Proceedings of the World Congress on Engineering **2** (2007).

[10] M. Sarıkaya, A. Güllü, Journal of Cleaner Production **91**, 347-357 (2015).

[11] D. Singh, P.V. Rao, Int. J. Adv. Manuf. Tech. **32** (11-12), 1115-1124 (2007).

[12] H. Ding, Y.C. Shin, Mach. Sci. Technol. **17** (2), 246-269 (2013).

[13] A.K. Sahoo, B. Sahoo, Measurement. **45** (8), 2153-2165 (2012).

[14] M. Sadílek, J. Dubský, Z. Sadílková, Z. Poruba, Perspectives in Science **7**, 357-363 (2016).

[15] D.G. Thakur, B. Ramamoorthy, L. Vijayaraghavan, Mater. Design **30** (5), 1718-1725 (2009).

[16] S. Pervaiz, A. Rashid, I. Deiab, M. Nicolescu, Mater. Manuf. Process. **29** (3), 219-252 (2014).

[17] C.H. Che Haron, A. Ginting, H. Arshad, J. Mater. Process. Technol. **185**, 77-82 (2007).

[18] J.G. Lima, R.F. Avila, A.M. Abrao, M. Faustino, J. Paulo Davim, J. Mater. Process. Tech. **169** (3), 388-395 (2005).

[19] D.K. Das, A.K. Sahoo, R. Das, B.C. Routara, Proc. Mat. Sci. **6**, 1351-1358 (2014).

[20] W.L. Liu, W.T. Chien, M.H. Jiang, W.J. Chen, J. Alloys Compd. **495**, 97-103 (2010).

[21] A. Palanisamy, T. Selvaraja and S. Sivasankaran, J. Mech. Sci. Technol. **31** (9), 4159-4165 (2017).

[22] A. Palanisamy, T. Selvaraj, S. Sivasankaran, Mater. Manuf. Process (2018), DOI:10.1080/10426914.2018.1424910 (In press).

[23] H.S. Jailani, A. Rajadurai, B. Mohan, A.S. Kumar, T. Sornakumar, Int. J. Adv. Manuf. Technol. **45**, 362-369 (2009).

[24] R. Suresh, S. Basavarajappa, V.N. Gaitonde, G.L. Samuel, Int. J. Refract. Met. H. **33**, 75-86 (2012).

[25] J. Deng, Introduction to Grey Theory, Journal of Grey Systems **1** (1), 1-24 (1989).

[26] P. Senthil, T. Selvaraj, K. Sivaprasad, Int. J. Adv. Manuf. Technol. **67** (5-8), 1589-1596 (2013).

[27] S.R. Das, D. Dhupal, A. Kumar, Measurement. **62**, 108-126 (2015).

[28] A. Pal, S.K. Choudhury, S. Chinchanikar, Proc. Mat. Sci. **6**, 80-91 (2014).

[29] Z.Z. Julie, C.C. Joseph, E. Daniel Kirby, J. Mater. Process. Technol. **184**, 233-239 (2007).

[30] L.K. Pan, C.C. Wang, S.L. Wei, H.F. Sher, J. Mater. Process. Technol, **182**, 107-116 (2007).

[31] D. Palanisamy, P. Senthil, V. Senthilkumar, Arch. Civ. Mech. Eng. **16** (1), 53-63 (2016).